ISSN 1070-3284, Russian Journal of Coordination Chemistry, 2015, Vol. 41, No. 10, pp. 644–653. © Pleiades Publishing, Ltd., 2015.
Original Russian Text © A.S. Zaeva, A.V. Ivanov, A.V. Gerasimenko, 2015, published in Koordinatsionnaya Khimiya, 2015, Vol. 41, No. 10, pp. 590–599.

Chemisorption Binding of Gold(III) from Solutions with Bismuth Dipropyldithiocarbamate: Supramolecular Self-Assembly (Role of the Secondary Au···S and Aurophilic Interactions) and Thermal Behavior of the Solvated Heteropolynuclear Ionic Type Complex $([Au\{S_2CN(C_3H_7)_2\}_2]_3[Bi_2Cl_9] \cdot 0.5CO(CH_3)_2 \cdot 0.5HCl)_n$

A. S. Zaeva[a], A. V. Ivanov[a], and A. V. Gerasimenko[b]

[a] *Institute of Geology and Nature Management, Far East Branch, Russian Academy of Sciences, Ryolochny Lane 1, Blagoveschensk, 675000 Russia*

[b] *Institute of Chemistry, Far East Branch, Russian Academy of Sciences, pr. Stoletiya Vladivostoka 159, Vladivostok, 690022 Russia*

e-mail: alexander.v.ivanov@chemist.com

Received February 25, 2015

Abstract—The reaction of binuclear bismuth(III) *N*,*N*-dipropyldithiocarbamate $[Bi_2\{S_2CN(C_3H_7)_2\}_6]$ with a solution of $AuCl_3$ in 2 M HCl was studied. Crystallization of the heterogeneous reaction products from an acetone solution afforded the polymeric solvated heteropolynuclear gold(III)–bismuth complex, $([Au\{S_2CN(C_3H_7)_2\}_2]_3[Bi_2Cl_9] \cdot 1/2CO(CH_3)_2 \cdot 1/2HCl)_n$ (**I**). According to X-ray diffraction data (CIF file CCDC no. 1050766), the structure of **I** comprises four isomeric $[Au\{S_2CN(C_3H_7)_2\}_2]^+$ cations in 1 : 1 : 2 : 2 ratio, namely: cation "A" with the Au(1) atom, cation "B" with the Au(2) atom, cation "C" with the Au(3) atom, and cation "D" with the Au(4) atom, and the discrete binuclear $[Bi_2Cl_9]^{3-}$ anions. The isomeric gold(III) complex cations are involved in the construction of two types of cationic triads, ["C"···"A"···"C"] and ["D"···"B"···"D"], through secondary bonds and short Au···S contacts. The cation types differ by both the nature of binding and the Au–Au distances. The weak aurophilic binding between the cationic triads (Au···Au 3.5416(2) Å) gives rise to zigzag-like polymeric chains $(\cdots["C"\cdots"A"\cdots"C"]\cdots["D"\cdots"B"\cdots"D"]\cdots)_n$ extended along the *y* axis. In turn, the $[Bi_2Cl_9]^{3-}$ anions located on one side of polymer chains are held by the secondary Cl···S bonds. The outer-sphere $CO(CH_3)_2$ and HCl solvate molecules joined by hydrogen bonds are located in the space between bismuth anions. The thermal behavior of **I** was studied by simultaneous thermal analysis. The thermal destruction of the complex includes desolvation and thermolysis of the dithiocarbamate moiety and $[Bi_2Cl_9]^{3-}$ with liberation of gold metal and bismuth chloride (which is subsequently evaporated) and partial formation of Bi_2S_3. In the temperature range of 712–828°C, bismuth sulfide is oxidized to $(BiO)_2SO_4$, which decomposes above 828°C to give Bi_2O_3. Bismuth(III) oxide and reduced gold are the final products of thermal transformations.

DOI: 10.1134/S1070328415090109

The recent interest in the chemistry of bismuth is due to the possibility to obtain structurally diverse complexes potentially suitable for a variety of applications. Indeed, organic-inorganic hybrid materials based on bismuth exhibit unusual optical, thermal, catalytic, and other properties [1–3]. Compounds containing bismuth halide complex anions exhibit promising ferroelectric characteristics [4–6]. Systems comprising bismuth halide anions in combination with organic cations demonstrate semiconductor properties [7]. The potential of practical applications of bismuth compounds with dialkyldithiocarbamate ligands is due to their high antitumor and antibacterial activities [8–11] and suitability as precursors of Bi_2S_3 nanopowders and films in chemical vapor deposition processes [12–17]. It was shown by recent studies that cadmium, zinc, bismuth, and thallium(I) dialkyldithiocarbamate complexes are able to efficiently preconcentrate gold(III) from solutions to give various polynuclear, heteropolynuclear, and heterovalent complexes as the individual gold binding species [18–25]. It is also noteworthy that Au(III) and Au(I) complexes with dithiocarbamate ligands behave as highly efficient new-generation anticancer drugs [26–29]. Thus, preparation and studies of structure and physicochemical properties of new gold(III) bismuth dithiocarbamate complexes are of considerable practical interest.

As a continuation of studies of species formed upon gold(III) binding with dithiocarbamate complexes from solutions of the reaction products of bismuth(III) *N*,*N*-dipropyldithiocarbamate (PDtc) with

a solution of $AuCl_3$ in 2 M HCl, the solvated bis(*N*,*N*-dipropyldithiocarbamato-*S*,*S*')gold(III) nonachlorodibismuthate $[Au\{S_2CN(C_3H_7)_2\}_2]_3[Bi_2Cl_9] \cdot 1/2CO(CH_3)_2 \cdot 1/2HCl$ (**I**) was preparatively isolated (by crystallization from acetone solution) and studied by X-ray diffraction and simultaneous thermal analysis (STA).

EXPERIMENTAL

The initial binuclear complex $[Bi_2\{S_2CN(C_3H_7)_2\}_6]$ (**II**) was prepared by the reaction between aqueous solutions of $Bi(NO_3)_3 \cdot 5H_2O$ (first dissolved in HNO_3) and $Na\{S_2CN(C_3H_7)_2\} \cdot H_2O$ taken above the stoichiometric amount (~15%)[1]. Complex **II** and the initial sodium dipropyldithiocarbamate hydrate were identified using the ^{13}C MAS NMR data (δ, ppm):

II: 203.6, 202.1, 200.9, 200.1 (6 : 5 : 4 : 3, $-S_2CN=$); 56.6, 56.1, 55.3 (3 : 2 : 1, $=NCH_2-$); 23.0, 21.6, 21.3, 20.9, 20.6, 20.1 (1 : 6 : 5 : 12 : 4 : 8, $-CH_2-$); 13.2, 13.0, 12.7, 12.3, 12.2, 11.8, 11.6 (1 : 5 : 7 : 4 : 7 : 6 : 6, $-CH_3$).

$Na\{S_2CN(C_3H_7)_2\} \cdot H_2O$: 208.3 ($-S_2CN=$); 59.4, 57.9 (1 : 1, $=NCH_2-$); 22.3, 21.5 (1 : 1, $-CH_2-$); 12.6, 11.5 (1 : 1, $-CH_3$).

Synthesis of $[Au\{S_2CN(C_3H_7)_2\}_2]_3[Bi_2Cl_9] \cdot 1/2CO(CH_3)_2 \cdot 1/2HCl$ (I). A solution of $AuCl_3$ in 2 M HCl (20 mL) containing 46.8 mg of gold was added to 200 mg of freshly precipitated bismuth dipropyldithiocarbamate **II** and the mixture was stirred for 1 h. The residual gold in the solution was determined by a Hitachi first class atomic absorption spectrometer, model 180-50. The resulting bright orange precipitate was filtered off, washed with water, and dried in the filter. The orange prismatic crystals of complex **I** for X-ray diffraction were obtained from solutions in acetone at room temperature.

X-Ray diffraction analysis was performed at 170(2) K for a prismatic single crystal on a BRUKER Kappa APEX II diffractometer (MoK_α radiation, $\lambda = 0.71073$ Å, graphite monochromator). The absorption corrections were applied by face indices of the single crystal. The structure was solved by the direct method and refined by the least squares method (on F^2) in the anisotropic approximation for non-hydrogen atoms. The positions of the hydrogen atoms were calculated geometrically and included in the refinement in the riding model. The hydrogen atom of the HCl molecule was not located.

The data were collected and edited and the unit cell parameters were refined using the APEX2 [31] and SAINT [32] program packages. All calculations on the structure solution and refinement were performed using the SHELXTL/PC program package [33]. The key crystallographic data and the structure refinement details are summarized in Table 1 and the bond lengths and bond angles are given in Table 2.

Table 1. Crystallographic data and X-ray experiment and structure refinement details for $[Au\{S_2CN(C_3H_7)_2\}_2]_3[Bi_2Cl_9] \cdot 1/2CO(CH_3)_2 \cdot 1/2HCl$ (**I**)

Parameter	Value
M	2433.05
System	Monoclinic
Space group	$P2_1/n$
a, Å	12.9905(3)
b, Å	21.8086(6)
c, Å	27.4182(7)
β, deg	90.9730(10)
V, Å^3	7766.6(3)
Z	4
ρ_{calcd}, g/cm^3	2.081
μ, mm–1	10.847
$F(000)$	4604
Crystal size, mm	$0.69 \times 0.31 \times 0.27$
Data collection range of θ, deg	1.72–34.37
Ranges of reflection indices	$-20 \le h \le 19$, $-34 \le k \le 34$, $-32 \le l \le 43$
Number of measured reflections	114288
Number of independent reflections	32080 ($R_{int} = 0.0333$)
Number of reflections with $I > 2\sigma(I)$	25689
Refinement method	Full-matrix least squares on F^2
Number of refinement parameters	730
GOOF	1.064
R-factors for $F^2 > 2\sigma(F^2)$	$R_1 = 0.0440$, $wR_2 = 0.1162$
R-factors for all reflections	$R_1 = 0.0591$, $wR_2 = 0.1217$
Extinction coefficient	Not refined
$\Delta\rho_{min}/\Delta\rho_{max}$, e Å^{-3}	–2.592/3.211

The atom coordinates, bond lengths, and bond angles are deposited with the Cambridge Crystallographic Data Centre (no. 1050766; deposit@ccdc.cam.ac.uk or http://www.ccdc.cam.ac.uk).

The thermal behavior of I was studied by STA with simultaneous recording of thermogravimetry (TG) and differential scanning calorimetry (DSC) curves. The measurements were performed on an STA 449C Jupiter NETZSCH instrument in corundum/aluminum crucibles covered with a lid containing a hole to maintain a pressure of 1 atm during the thermal

[1] Sodium *N*,*N*-dipropyldithiocarbamate was prepared by the reaction between dipropylamine and carbon disulfide (Merck) in an alkaline medium [30]

Table 2. Selected bond lengths (*d*) and bond (ω) and torsion (φ) angles in structure **I***

Cation "A"		Cation "B"	
Bond	*d*, Å	Bond	*d*, Å
Au(1)–S(1)	2.3205(6)	Au(2)–S(3)	2.3272(7)
Au(1)–S(2)	2.3275(7)	Au(2)–S(4)	2.3343(7)
S(1)–C(1)	1.741(3)	Au(2)···S(11)	3.9953(7)
S(2)–C(1)	1.724(3)	Au(2)···S(12)	4.0019(7)
N(1)–C(1)	1.293(3)	S(3)–C(8)	1.732(3)
N(1)–C(2)	1.480(4)	S(4)–C(8)	1.731(3)
N(1)–C(5)	1.476(3)	N(2)–C(8)	1.299(4)
		N(2)–C(9)	1.486(4)
		N(2)–C(12)	1.476(4)
Angle	ω, deg	Angle	ω, deg
S(1)Au(1)S(2)	75.52(2)	S(3)Au(2)S(4)	75.34(2)
S(1)Au(1)S(2)[a]	104.48(2)	S(3)Au(2)S(4)[b]	104.66(2)
C(1)S(1)Au(1)	86.90(9)	C(8)S(3)Au(2)	87.06(10)
C(1)S(2)Au(1)	87.08(9)	C(8)S(4)Au(2)	86.87(10)
S(1)C(1)S(2)	110.47(14)	S(3)C(8)S(4)	110.7(2)
S(1)C(1)N(1)	124.2(2)	S(3)C(8)N(2)	124.1(2)
S(2)C(1)N(1)	125.4(2)	S(4)C(8)N(2)	125.2(2)
C(1)N(1)C(2)	120.6(2)	C(8)N(2)C(9)	121.8(2)
C(1)N(1)C(5)	122.2(2)	C(8)N(2)C(12)	121.2(2)
Angle	φ, deg	Angle	φ, deg
Au(1)S(1)S(2)C(1)	−178.0(2)	Au(2)S(3)S(4)C(8)	177.4(2)
S(1)Au(1)C(1)S(2)	−178.20(14)	S(3)Au(2)C(8)S(4)	177.7(2)
S(1)C(1)N(1)C(2)	179.6(2)	S(3)C(8)N(2)C(9)	176.5(2)
S(1)C(1)N(1)C(5)	−2.7(4)	S(3)C(8)N(2)C(12)	−3.3(4)
S(2)C(1)N(1)C(2)	−1.0(4)	S(4)C(8)N(2)C(9)	−2.5(4)
S(2)C(1)N(1)C(5)	176.7(2)	S(4)C(8)N(2)C(12)	177.7(2)
Cation "C"		Cation "D"	
Bond	*d*, Å	Bond	*d*, Å
Au(3)–S(5)	2.3296(6)	Au(4)–S(9)	2.3363(7)
Au(3)–S(6)	2.3352(6)	Au(4)–S(10)	2.3324(7)
Au(3)–S(7)	2.3417(6)	Au(4)–S(11)	2.3350(7)
Au(3)–S(8)	2.3381(7)	Au(4)–S(12)	2.3244(7)
Au(3)···S(1)	3.4919(7)	Au(4)···S(3)[b]	3.9150(8)
S(5)–C(15)	1.732(3)	Au(4)···S(4)	3.8813(7)
S(6)–C(15)	1.727(3)	S(9)–C(29)	1.725(3)
S(7)–C(22)	1.727(3)	S(10)–C(29)	1.726(3)
S(8)–C(22)	1.723(3)	S(11)–C(36)	1.731(3)
N(3)–C(15)	1.304(3)	S(12)–C(36)	1.731(3)
N(4)–C(22)	1.319(3)	N(5)–C(29)	1.306(3)
N(3)–C(16)	1.474(3)	N(6)–C(36)	1.292(3)
N(3)–C(19)	1.483(4)	N(5)–C(30)	1.456(4)
N(4)–C(23)	1.484(3)	N(5)–C(33)	1.490(4)
N(4)–C(26)	1.475(3)	N(6)–C(37)	1.487(3)
		N(6)–C(40)	1.452(4)
Angle	ω, deg	Angle	ω, deg
S(5)Au(3)S(6)	75.41(2)	S(9)Au(4)S(10)	75.16(2)
S(5)Au(3)S(7)	179.55(3)	S(9)Au(4)S(11)	106.14(2)
S(5)Au(3)S(8)	104.22(2)	S(9)Au(4)S(12)	176.77(3)
S(6)Au(3)S(7)	104.87(2)	S(10)Au(4)S(11)	178.69(2)
S(6)Au(3)S(8)	177.98(3)	S(10)Au(4)S(12)	103.34(3)
S(7)Au(3)S(8)	75.48(2)	S(11)Au(4)S(12)	75.36(2)
C(15)S(5)Au(3)	86.71(8)	C(29)S(9)Au(4)	86.71(10)
C(15)S(6)Au(3)	86.64(8)	C(29)S(10)Au(4)	86.80(9)

Table 2. (Contd.)

Cation "C"		Cation "D"	
Angle	ω, deg	Angle	ω, deg
C(22)S(7)Au(3)	86.01(9)	C(36)S(11)Au(4)	86.80(9)
C(22)S(8)Au(3)	86.20(9)	C(36)S(12)Au(4)	87.13(9)
S(5)C(15)S(6)	111.17(13)	S(9)C(29)S(10)	111.2(2)
S(7)C(22)S(8)	112.26(14)	S(11)C(36)S(12)	110.7(2)
S(5)C(15)N(3)	124.1(2)	S(9)C(29)N(5)	125.1(2)
S(6)C(15)N(3)	124.8(2)	S(10)C(29)N(5)	123.7(2)
S(7)C(22)N(4)	123.4(2)	S(11)C(36)N(6)	125.2(2)
S(8)C(22)N(4)	124.4(2)	S(12)C(36)N(6)	124.1(2)
C(15)N(3)C(16)	121.5(2)	C(29)N(5)C(30)	122.3(3)
C(15)N(3)C(19)	120.3(2)	C(29)N(5)C(33)	119.4(2)
C(22)N(4)C(23)	121.5(2)	C(36)N(6)C(37)	121.5(2)
C(22)N(4)C(26)	121.7(2)	C(36)N(6)C(40)	121.8(2)
Angle	φ, deg	Angle	φ, deg
Au(3)S(5)S(6)C(15)	176.8(2)	Au(4)S(9)S(10)C(29)	175.9(2)
S(5)Au(3)C(15)S(6)	177.16(13)	S(9)Au(4)C(29)S(10)	176.33(14)
Au(3)S(7)S(8)C(22)	−177.7(2)	Au(4)S(11)S(12)C(36)	−178.7(2)
S(7)Au(3)C(22)S(8)	−177.95(14)	S(11)Au(4)C(36)S(12)	−178.86(14)
S(5)C(15)N(3)C(16)	6.4(3)	S(9)C(29)N(5)C(30)	−179.5(2)
S(5)C(15)N(3)C(19)	−174.6(2)	S(9)C(29)N(5)C(33)	2.8(4)
S(6)C(15)N(3)C(16)	−173.9(2)	S(10)C(29)N(5)C(30)	1.1(4)
S(6)C(15)N(3)C(19)	5.1(3)	S(10)C(29)N(5)C(33)	−176.6(2)
S(7)C(22)N(4)C(23)	179.0(2)	S(11)C(36)N(6)C(37)	−176.5(2)
S(7)C(22)N(4)C(26)	0.5(4)	S(11)C(36)N(6)C(40)	−2.5(4)
S(8)C(22)N(4)C(23)	−1.8(4)	S(12)C(36)N(6)C(37)	1.1(4)
S(8)C(22)N(4)C(26)	179.6(2)	S(12)C(36)N(6)C(40)	175.1(2)
$[Bi_2Cl_9]^{3-}$ complex anion			
Bond	*d*, Å	Bond	*d*, Å
Bi(1)−Cl(1)	2.8783(8)	Bi(2)−Cl(1)	2.8936(8)
Bi(1)−Cl(2)	2.9867(9)	Bi(2)−Cl(2)	2.8888(9)
Bi(1)−Cl(3)	2.8872(7)	Bi(2)−Cl(3)	2.8313(7)
Bi(1)−Cl(4)	2.5421(7)	Bi(2)−Cl(7)	2.6165(7)
Bi(1)−Cl(5)	2.5941(8)	Bi(2)−Cl(8)	2.5909(8)
Bi(1)−Cl(6)	2.5726(7)	Bi(2)−Cl(9)	2.6028(8)
Angle	ω, deg	Angle	ω, deg
Cl(1)Bi(1)Cl(2)	76.26(2)	Cl(1)Bi(2)Cl(7)	169.61(2)
Cl(1)Bi(1)Cl(3)	79.33(2)	Cl(1)Bi(2)Cl(8)	91.48(2)
Cl(1)Bi(1)Cl(4)	91.95(2)	Cl(1)Bi(2)Cl(9)	95.60(3)
Cl(1)Bi(1)Cl(5)	169.23(2)	Cl(2)Bi(2)Cl(3)	80.98(2)
Cl(1)Bi(1)Cl(6)	95.18(2)	Cl(2)Bi(2)Cl(7)	99.33(3)
Cl(2)Bi(1)Cl(3)	78.43(2)	Cl(2)Bi(2)Cl(8)	167.98(3)
Cl(2)Bi(1)Cl(4)	160.48(2)	Cl(2)Bi(2)Cl(9)	94.57(3)
Cl(2)Bi(1)Cl(5)	94.80(2)	Cl(3)Bi(2)Cl(7)	89.75(2)
Cl(2)Bi(1)Cl(6)	103.09(3)	Cl(3)Bi(2)Cl(8)	92.31(2)
Cl(3)Bi(1)Cl(4)	84.18(2)	Cl(3)Bi(2)Cl(9)	174.29(3)
Cl(3)Bi(1)Cl(5)	93.13(2)	Cl(7)Bi(2)Cl(8)	90.56(3)
Cl(3)Bi(1)Cl(6)	173.85(2)	Cl(7)Bi(2)Cl(9)	94.53(2)
Cl(4)Bi(1)Cl(5)	94.93(2)	Cl(8)Bi(2)Cl(9)	91.43(3)
Cl(4)Bi(1)Cl(6)	93.31(3)	Bi(1)Cl(1)Bi(2)	86.02(2)
Cl(5)Bi(1)Cl(6)	92.68(3)	Bi(1)Cl(2)Bi(2)	84.14(2)
Cl(1)Bi(2)Cl(2)	77.58(2)	Bi(1)Cl(3)Bi(2)	87.02(2)
Cl(1)Bi(2)Cl(3)	80.00(2)		

* Symmetry codes: [a] $-x+2, -y+1, -z+2$; [b] $-x+2, -y, -z+2$.

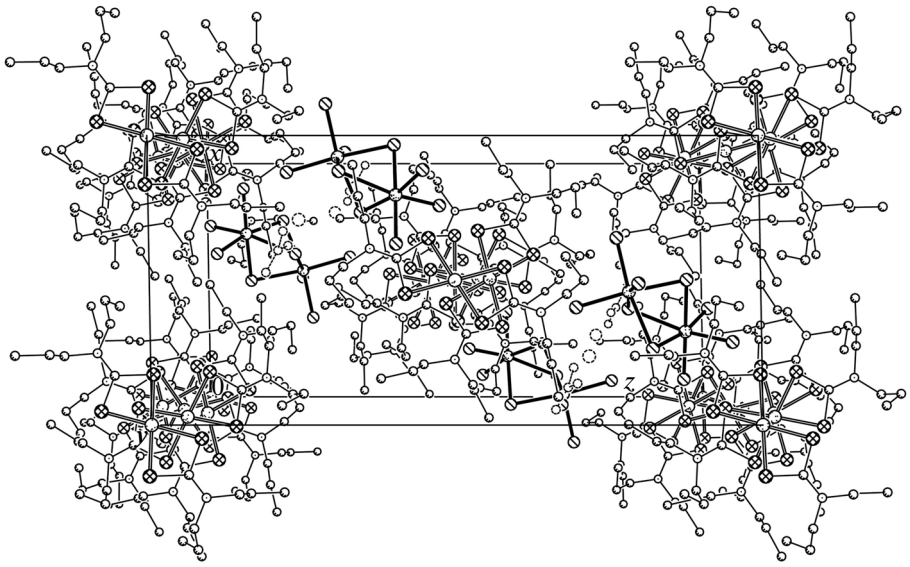

Fig. 1. Projection of structure **I** on the *xz* plane. The polymer chains are extended along the *y* direction.

decomposition of the sample. The samples were heated under argon up to 1100/600°C at a rate of 5/10°C/min. The sample weight was 2.138–3.730 mg. The accuracy of temperature measurement was ±0.7°C, that of the mass change was $\pm 1 \times 10^{-4}$ mg. After thermal analysis, the residual substance was examined with a JSM 6390LV JEOL scanning electron microscope (Japan) equipped with an Oxford INCA Energy 350-Wave microanalysis system (UK) with energy and wavelength dispersion. The qualitative determination of the chemical composition was performed by the microprobe method using an energy dispersive spectrometer. The independent determination of the melting point of the complex was done in a capillary using an PTP(M) instrument (OJSC Khimlaborpribor).

RESULTS AND DISCUSSION

The reaction between freshly precipitated binuclear complex **II** and a solution of $AuCl_3$ in 2 M HCl is accompanied by fast transformation of the voluminous yellow flaky precipitate of the chemosorbent involving color change to bright orange, a decrease in the particle size and a change in the particle shape to rounded. Simultaneously, the working solution is decolorized, the degree of binding of gold by the precipitate being 98.9%. These changes are due to the formation of new compounds in the system. The reaction of bismuth(III) dipropyldithiocarbamate with a solution of gold(III) is reduced to gold binding and can be represented as follows:

$$[Bi_2\{S_2CN(C_3H_7)_2\}_6] + 3H[AuCl_4] = [Au\{S_2CN(C_3H_7)_2\}_2]_3[Bi_2Cl_9] + 3HCl.$$
(II) **(I)**

The unit cell of **I** contains four formula units of $[Au\{S_2CN(C_3H_7)_2\}_2]_3[Bi_2Cl_9] \cdot 1/2CO(CH_3)_2 \cdot 0.5HCl$ (Fig. 1). The $[Au\{S_2CN(C_3H_7)_2\}_2]^+$ complex cations exhibit structural non-equivalence: among the twelve gold(III) cations in the unit cell, there are two centrosymmetric cations "A" with Au(1), two centrosymmetric cations "B" with Au(2), four non-centrosymmetric cations "C" with Au(3), and four non-centrosymmetric cations "D" with Au(4) (Table 2, Fig. 2).

In each of the $[Au\{S_2CN(C_3H_7)_2\}_2]^+$ cations, the gold atom coordinates two *S*,*S*'-bidentate PDtc ligands. The narrow range of Au–S bond lengths (2.3205–2.3417 Å) determines a nearly isobidentate coordination of PDtc ligands. This coordination mode results in the formation of a metal environment of four sulfur atoms: the diagonal SAuS angles in the $[AuS_4]$ chromophores are 180° or close to 180° (Table 2); this corresponds to a low-spin intraorbital dsp^2 hybrid state of gold. Each cation contains two small-size nearly planar (the AuSSC and SAuCS torsion angles do not considerably deviate from 180°) four-membered $[AuS_2C]$ metal rings formed upon bidentate chelating coordination of the PDtc ligands, which share a gold atom to give a bicyclic fragment, $[CS_2AuS_2C]$. The distances between gold and carbon

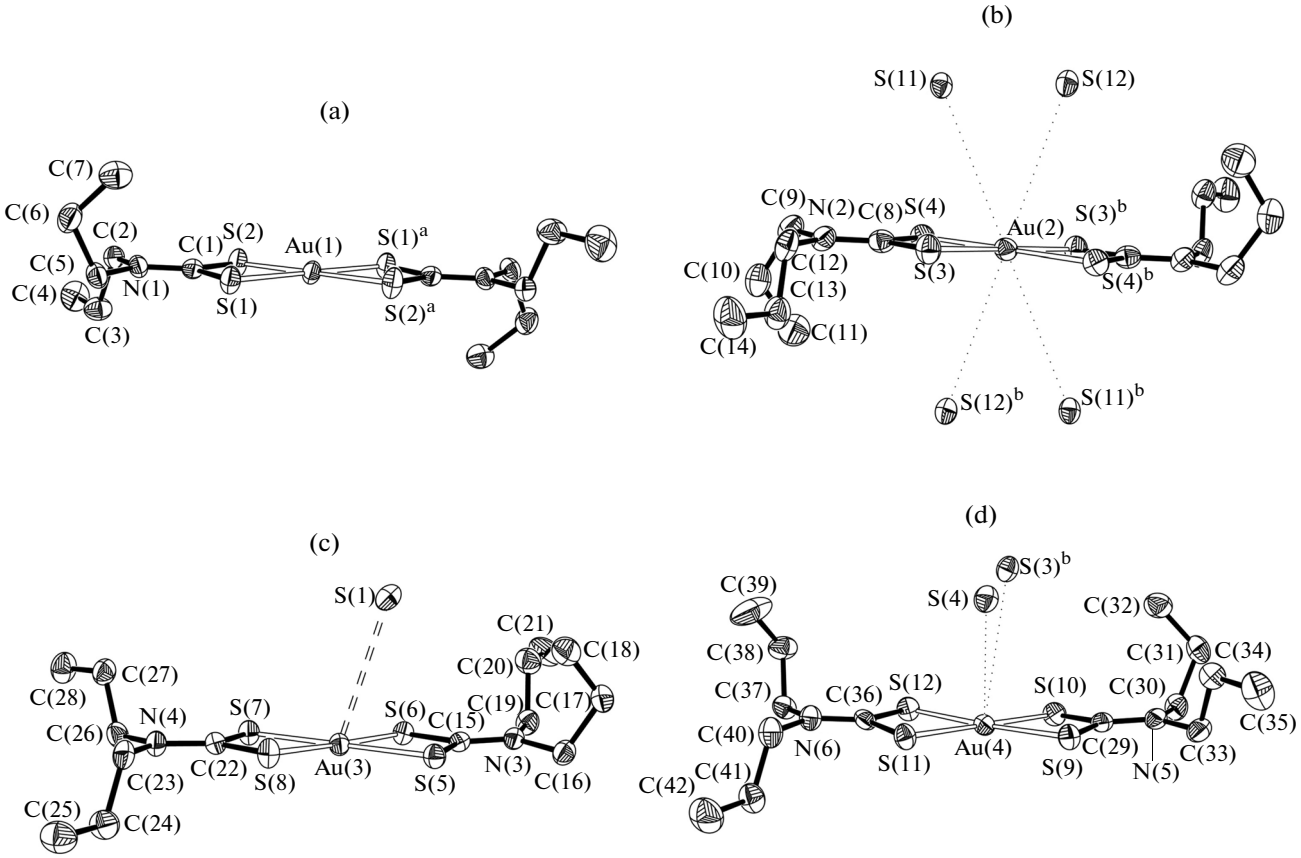

Fig. 2. Structure of isomeric complex cations $[Au\{S_2CN(C_3H_7)_2\}_2]^+$: (a) "A", (b) "B", (c) "C", and (d) "D" (50% probability ellipsoids). The secondary bonds and short Au···S contacts between the neighboring cations are shown by double dashed lines and dotted lines, respectively.

atoms *trans*-oriented in the rings are in the range of 2.811–2.829 Å, which is much smaller than the sum of van der Waals radii of these atoms (3.36 Å) [34, 35]. This attests to the existence of transannular interaction between them and the presence of high concentration of π-electron density inside the rings.

The CNCS torsion angles close to 0° or 180° (Table 2) reflect the planar structure of the $C_2NC(S)S$ structural fragments; only the C(16) and C(19) atoms in cation "C" have significant deviations from the plane. The noticeably stronger N–C(S)S bonds (1.292–1.319 Å) in the dipropyldithiocarbamate ligands as compared with the $N–CH_2$ bonds (1.452–1.490 Å) attest to a contribution of double bonding to these formally single bonds and admixture of the sp^2- to sp^3 hybrid state of the corresponding nitrogen and carbon atoms. The structural differences between non-equivalent complex cations "A", "B", "C", and "D" (Table 2) allow them to be classified as conformers.

The anionic part of compound **I** is formed by the discrete $[Bi_2Cl_9]^{3-}$ complex ion (Fig. 3, Table 2). Around each of the two Bi atoms, six chlorine atoms form a distorted octahedral environment. The $[BiCl_6]$ octahedra are combined into a binuclear complex anion by sharing a face defined by three μ_2-brinding Cl(1), Cl(2), and Cl(3) atoms. For the most strongly bound terminal chlorine atoms, the Bi–Cl distances are in the range of 2.5421–2.6165 Å. The bridging Bi–Cl bonds are much longer (2.8313–2.9867 Å). The

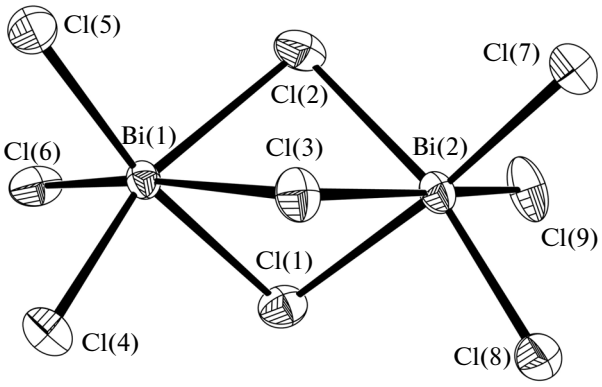

Fig. 3. Structure of the complex anion $[Bi_2Cl_9]^{3-}$ (50% probability ellipsoids).

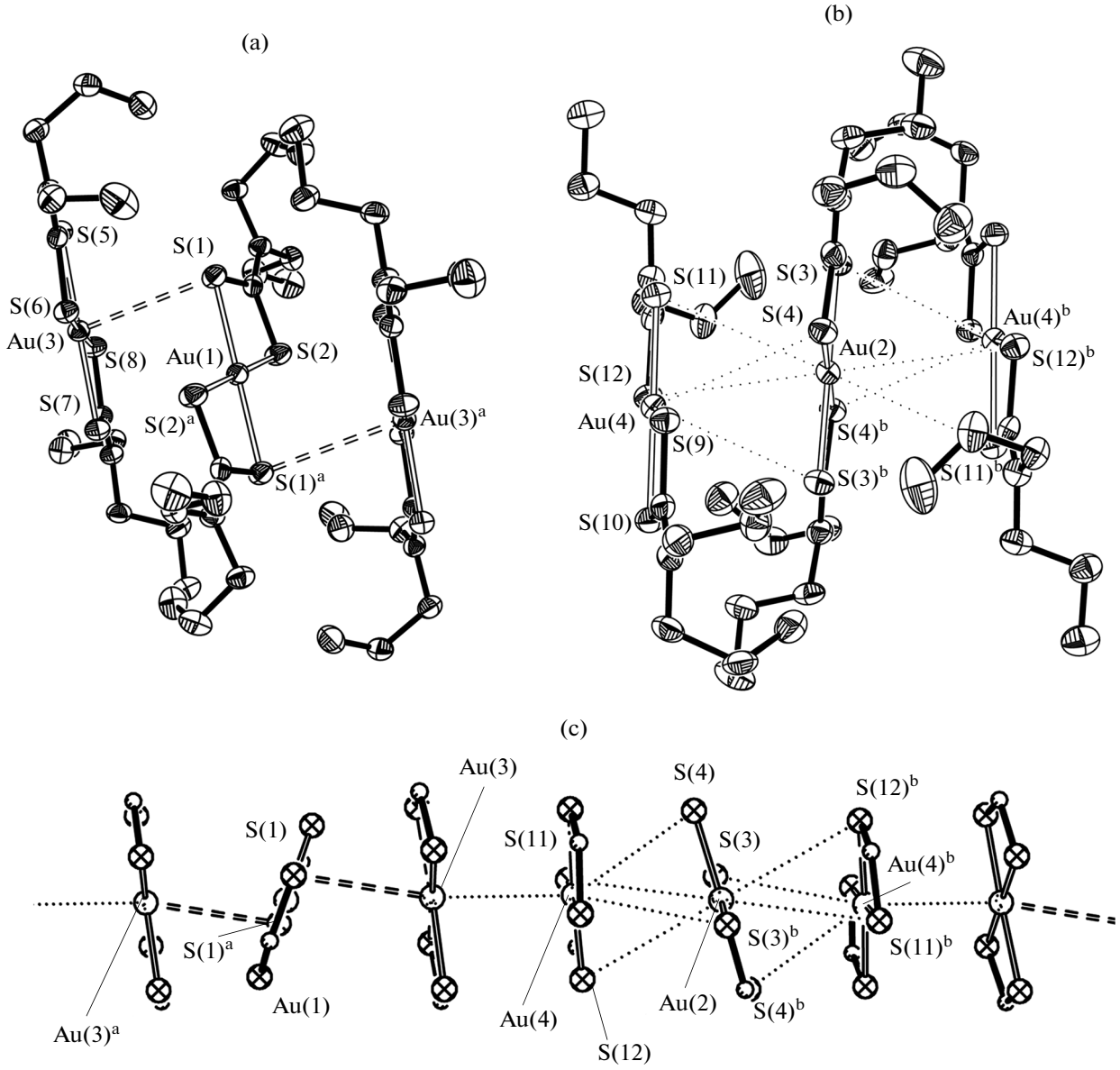

Fig. 4. Structure of the cationic triads (a) ["C"···"A"···"C"]$^{3+}$ and (b) ["D"···"B"···"D"]$^{3+}$. (c) Pattern of the polymer chain (···["C"···"A"···"C"]···["D"···"B"···"D"]···)$_n$ in complex **I**. The double dashed lines show the secondary Au···S bonds and the dotted lines show short Au···S contacts and aurophilic Au···Au bonds.

Bi···Bi distance of 3.9373(2) Å is consistent with published data [36–38].

The structural self-organization of compound **I** at the supramolecular level is due to relatively weak nonvalence Au···S contacts (short contacts and secondary bonds [39]) between the isomeric $[Au\{S_2CN(C_3H_7)_2\}_2]^+$ cations. The cations being discussed form linear trinuclear structural fragments $[Au_3\{S_2CN(C_3H_7)_2\}_6]^{3+}$ of two types: ["C"···"A"···"C"] and ["D"···"B"···"D"]; the Au(3)···Au(1)···Au(3)^a and Au(4)···Au(2)···Au(4)^b angles are 180° (Table 2). In the "C"–"C" and "D"–"D" pairs, the non-centrosymmetric cations have antiparallel orientation (Fig. 4). In the ["C"···"A"···"C"] cationic triad, the complex cations are combined by secondary Au(3)···S(1) and Au(3)^a···S(1)^a bonds (3.4919 Å, which is close to the sum of the van der Waals radii of gold and sulfur of 3.46 Å [34, 35]). Thus, the Au(3) atom occurs in the distorted tetragonal pyramidal [AuS_5] environment (Fig. 4a); the Au(1)···Au(3) distance is 4.02052(13) Å. In the second triad, ["D"···"B"···"D"] (Fig. 4b), the Au(2) atom of cation "B" forms two pairs of symmetric short Au···S contacts with the sulfur atoms of one PDtc ligand of cations "D": Au(2)···S(12), Au(2)···S(12)^b 4.0019 Å; and Au(2)···S(11), Au(2)···S(11)^b 3.9953 Å. (The [AuS_8] polyhedron can be approximated by a highly distorted tetragonal

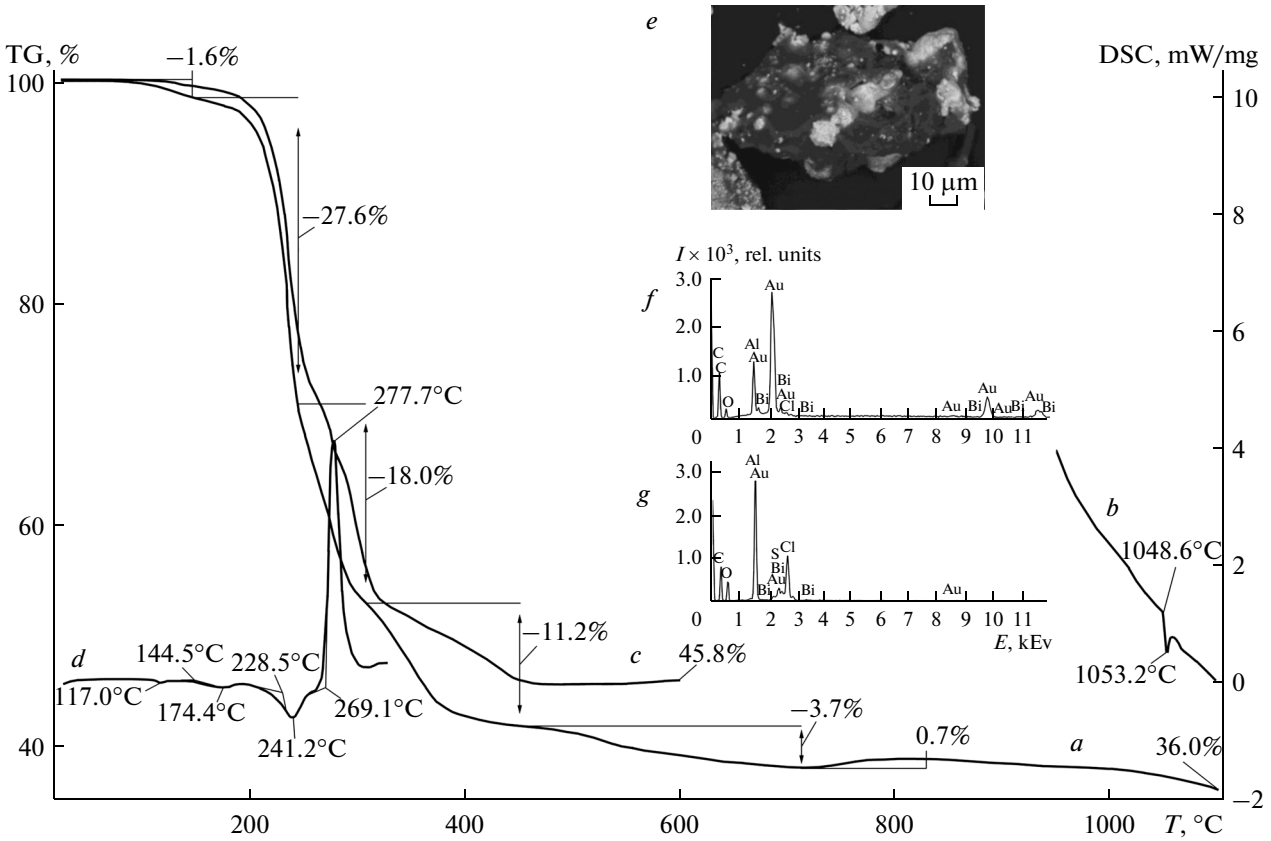

Fig. 5. (*a*, *c*) TG and (*b*, *d*) DSC curves of complex **I** in the (*a*, *b*) corundum and (*c*, *d*) aluminum crucibles. (*e*) Image of residual substance particles in the aluminum crucible and (*f*, *g*) energy dispersive X-ray spectra of (*f*) light and (*g*) dark areas.

prism.) Additionally, the Au(4) gold atom in each cation "D" has two short contacts with the sulfur atoms of two PDtc ligands of cation "B" (Au(4)···S(4) 3.8813 Å; Au(4)···S(3)^b 3.9150 Å), thus forming a distorted trigonal prismatic $[AuS_6]$ polyhedron in which the central gold atom occurs virtually in the S(9)S(10)S(11)S(12) plane. This intricate fashion of structural ordering in the trinuclear ["D"···"B"···"D"] moiety leads to shortening of the Au(2)···Au(4) distance to 3.88987(14) Å. The aurophilic interaction [40–42] between the cationic triads (Au(3)···Au(4) 3.5416(2) Å) gives rise to zigzag-like polymeric chains (···["C"···"A"···"C"]··· ["D"···"B"···"D"]···)$_n$ extended along the *y* axis (Fig. 1): the Au(1)···Au(3)···Au(4) and Au(2)···Au(4)···Au(3) angles are 147.880° and 171.167°, respectively (Fig. 4). The polymeric chains being discussed are involved in the interaction with discrete binuclear bismuth anions, $[Bi_2Cl_9]^{3-}$, through the secondary bonds (Cl···S [43, p. 266]: Cl(9)···S(5) $(-1/2+x, 1/2-y, -1/2+z)$ 3.174(1) Å, Cl(4)···S(9) $(x, y, -1+z)$ 3.256(1) Å, Cl(4)···S(11) $(x, y, -1+z)$ 3.176(1) Å), which are markedly shorter than the sum of the van der Waals radii of chlorine and sulfur atoms (3.55 Å) [34, 35]). The $CO(CH_3)_2$ and HCl solvate molecules are arranged in the space between the discrete $[Bi_2Cl_9]^{3-}$ anions.

Note that the complex $[Au\{S_2CN(C_3H_7)_2\}_2]_3[Bi_3Cl_{12}]$ (**III**) distinguished by unusual geometry of the tribismuth complex anion, which was reported in our previous work [24], is characterized by a similar pattern of zigzag-like polymeric chains. In complex **III**, the $[Bi_3Cl_{12}]^{3-}$ anion having an angular structure (the Bi(1)Bi(2)Bi(3) angle of 72.358°) instead of the usual linear structure was detected for the first time. Comparison of the structural characteristics of complexes **I** (Table 2) and **III** provides the conclusion that the presence of outer-sphere solvate molecules in the former complex results in weakening of secondary (Au···S) and aurophilic (Au···Au) non-valence bonds.

The thermal behavior of **I** was studied by STA (simultaneous recording of TG and DSC curves) under argon. The TG curve (Fig. 5a) shows the onset of weight loss as soon as at 92°C (1.6%); this was attributed to desorption of weakly bound solvate molecules, $CO(CH_3)_2$ and HCl (1.94% calcd.). The thermal destruction of the dithiocarbamate part of the complex is shown by two sections of the TG curve: (a) in the temperature range of 145–244°C, destruction of one of the PDtc ligands in the $[Au\{S_2CN(C_3H_7)_2\}_2]^+$

cations with desorption of the products (27.6% exp; 27.83% calcd.) and b) subsequent thermolysis with gold(III) reduction to the metal at 244–307°C. The latter process is accompanied by liberation of $BiCl_3$ and partial formation of bismuth sulfide (at the anion). According to calculations of the TG curve, upon thermolysis, 43% of bismuth evolve as $BiCl_3$ and 57% form the sulfide.[2] Therefore, the next stage in the temperature range of 307–450°C is due to evaporation of bismuth chloride (b.p. = 441°C [45]) and is accompanied by a weight loss of 11.2% (11.14% calcd.).

At 450°C, the TG curve arrives at the slightly sloping region of gradual desorption of other thermolysis products, and by 712°C, the residual weight (37.9%) corresponds to the reduced gold metal and formed Bi_2S_3 (36.34% calcd.) with some pyrolysis products of the organic part of the complex. At 828°C, the TG curve shows a weigh increment (0.7%) due to oxidation of Bi_2S_3 by oxygen impurity present in argon to give $(BiO)_2SO_4$ [46] (0.75% calcd.).

The high-temperature region of the TG curve (828–1100°C) reflects the weight loss due to decomposition of $(BiO)_2SO_4$ to bismuth oxide Bi_2O_3 [47]. The weight of the residue after completion of the thermolysis of 36.0% (calcd. 35.21%) was due to the reduced gold and Bi_2O_3. Some excess of the experimental weight of the residue may be related to the bismuth metal impurity in the reduced gold. (Partial reduction of Bi_2S_3 to the metal under inert atmosphere was noted previously [48]). This assumption is supported by the sharp decrease in the extrapolated m.p. of gold to 1048.6°C (Fig. 5*b*) (m.p. = 1064.43°C [45]). After completion of thermolysis, small gold beads framed by lemon-yellow Bi_2O_3 spots are found on the bottom of the crucible.

When corundum crucibles are used, the DSC curve does not show any significant heat effects in the low-temperature region. Therefore, the thermal behavior of **I** was additionally studied in aluminum crucibles (Figs 5*c*, 5*d*). For correct interpretation of the DSC curve, the melting point of **I** was determined by an independent method in a glass capillary. At 100°C, the color of the sample of **I** changes to reddish and gradually deepens to brick-red (at 130°C). The corresponding feebly pronounced endotherm in the DSC curve with an extremum at 117°C (Fig. 5*d*) reflects desolvation. Melting of **I** accompanied by decomposition occurs in a broad temperature range (140–164°C), which corresponds to the presence of a diffuse endotherm with a peak at 174.4°C in the DSC curve (extrapolated m.p. = 144.5°C).

The endotherm at 241.2°C corresponds to the initial stage of thermolysis of complex **I** (involving the first dithiocarbamate group in each complex cation $[Au\{S_2CN(C_3H_7)_2\}_2]^+$) with desorption of decomposition products (27.6% exp; 27.83% calcd.). A intense exotherm with a peak at 277.7°C (the extrapolated temperature of the process onset is 269.1°C) is related to the reduction of bismuth(III) to the metal via the reaction with aluminum forming the crucible [48]. Therefore, the pattern of TG curve is also substantially different in this temperature range (Fig. 5*c*).

After completion of the thermolysis, caverns and flowed sites were detected in the inner surface of the aluminum crucible (indicating the presence of a reaction with the sample) and a sintered black-colored lump with light brown inclusions was found on the crucible bottom. Under magnification, one can see that the inclusions are irregularly shaped bulky particles distributed in the dark uniform lump (Fig. 5*e*).

The energy-dispersive X-ray spectra reveal predominance of gold with bismuth, aluminum, chlorine, carbon, and oxygen impurities in the light areas (Fig. 5*f*). The dark areas tend to contain predominantly aluminum and chlorine together with bismuth and minor amounts of gold, sulfur, and oxygen (Fig. 5*g*). Thus, thermolysis of **I** in an aluminum crucible involves reduction of gold and bismuth to the metals (contaminated by the products of pyrolysis and aluminothermic process: the residual weight is 45.8%; the calculated value is 41.88%).

[2] In [44], the formation of metal sulfides upon thermolysis of complexes with sulfur-containing ligands was interpreted from the thermodynamic standpoint.

ACKNOWLEDGMENTS

This work was partially supported by the Presidium of the Far East Branch of the RAS, project nos. 15-I-3-001 and 15-II-3-001).

REFERENCES

1. Wu, L.-M., Wu, X.-T., and Chen, L., *Coord. Chem. Rev.*, 2009, vol. 253, nos 23–24, p. 2787.
2. Louvain, N., Mercier, N., and Boucher, F., *Inorg. Chem.*, 2009, vol. 48, no. 3, p. 879.
3. Hrizi, C., Samet, A., Abid, Y., et al., *J. Mol. Struct.*, 2011, vol. 992, nos 1–3, p. 96.
4. Jakubas, R., Piecha, A., Pietraszko, A., and Bator, G., *Phys. Rev.*, 2005, vol. B72, no. 10, p. 104107.
5. Piecha, A., Bia[illegible]óska, A., and Jakubas, R., *J. Phys.: Condens. Matter,* 2008, vol. 20, no. 32, comm. 325224.
6. Bi, W., Leblanc, N., Mercier, N., et al., *Chem. Mater.*, 2009, vol. 21, no. 18, p. 4099.
7. Zhu, X.H., Mercier, N., Frere, P., et al., *Inorg. Chem.*, 2003, vol. 42, no. 17, p. 5330.
8. Li, H., Lai, C.S., Wu, J., et al., *J. Inorg. Biochem.*, 2007, vol. 101, no. 5, p. 809.
9. Ishak, D.H.A., Ooi, K.K., Ang, K.-P., et al., *J. Inorg. Biochem.*, 2014, vol. 130, p. 38.
10. Ozturk, I.I., Banti, C.N., Kourkoumelis, N., et al., *Polyhedron*, 2014, vol. 67, p. 89.
11. Jamaluddin, N.A., Baba, I., and Ibrahim, N., *Malays. J. Anal. Sci*, 2014, vol. 18, no. 2, p. 251.

12. Nomura, R., Kanaya, K., and Matsuda, H., *Bull. Chem. Soc. Jpn.*, 1989, vol. 62, no. 3, p. 939.
13. Marino, G., Chierice, G.O., Pinheiro, C.D., and Souza, A.G., *Thermochim. Acta*, 1999, vol. 328, nos. 1–2, p. 209.
14. Monteiro, O.C., Nogueira, H.I.S., Trindade, T., and Motevalli, M., *Chem. Mater.*, 2001, vol. 13, no. 6, p. 2103.
15. Zhang, H., Huang, J., Zhou, X., and Zhong, X., *Inorg. Chem.*, 2011, vol. 50, no. 16, p. 7729.
16. Cabrita, J.F., Ferreira, V.C., and Monteiro, O.C., *Electrochim. Acta*, 2014, vol. 135, p. 121.
17. Sivasekar, S., Ramalingam, K., Rizzoli, C., and Alexander, N., *Inorg. Chim. Acta*, 2014, vol. 419, p. 82.
18. Rodina, T.A., Ivanov, A.V., Gerasimenko, A.V., et al., *Polyhedron*, 2012, vol. 40, no. 1, p. 53.
19. Rodina, T.A., Ivanov, A.V., and Gerasimenko, A.V., *Russ. J. Coord. Chem.*, 2014, vol. 40, no. 2, p. 100.
20. Ivanov, A.V., Rodina, T.A., and Loseva, O.V., *Russ. J. Coord. Chem.*, 2014, vol. 40, no. 12, p. 875.
21. Ivanov, A.V., Loseva, O.V., Rodina, T.A., et al., *Russ. J. Inorg. Chem.,* 2014, vol. 59, no. 8, p. 807.
22. Loseva, O.V. and Ivanov, A.V., *Russ. J. Inorg. Chem.*, 2014, vol. 59, no. 12, p. 1491.
23. Loseva, O.V., Rodina, T.A., Smolentsev, A.I., and Ivanov, A.V., *J. Struct. Chem.* 2014, vol. 55, no. 5, p. 901.
24. Zaeva, A.S., Ivanov, A.V., Gerasimenko, A.V., and Sergienko, V.I., *Russ. J. Inorg. Chem.*, 2015, vol. 60, no. 2, p. 203.
25. Ivanov, A.V., Bredyuk, O.A., Loseva, O.V., and Rodina, T.A., *Russ. J. Coord. Chem.*, 2015, vol. 41, no. 2, p. 108.
26. Ronconi, L., Giovagnini, L., Marzano, C., et al., *Inorg. Chem.*, 2005, vol. 44, no. 6, p. 1867.
27. Boscutti, G., Feltrin, L., Lorenzon, D., et al., *Inorg. Chim. Acta*, 2012, vol. 393, p. 304.
28. Keter, F.K., Guzei, I.A., Nell, M., et al., *Inorg. Chem.*, 2014, vol. 53, no. 4, p. 2058.
29. Shi, Y., Chu, W., Wang, Y., et al., *Inorg. Chem. Commun.*, 2013, vol. 30, p. 178.
30. Byr'ko, V.M., *Ditiokarbamaty* (Dithiocarbamates), Moscow: Nauka, 1984.
31. *APEX2,* Madison (WI): Bruker AXS, 2010.
32. *SAINT,* Madison (WI): Bruker AXS, 2010.
33. Sheldrick, G.M., *Acta Crystallogr., Sect. A: Found. Crystallogr.*, 2008, vol. 64, no. 1, p. 112.
34. Bondi, A., *J. Phys. Chem.*, 1964, vol. 68, no. 3, p. 441.
35. Bondi, A., *J. Phys. Chem.*, 1966, vol. 70, no. 9, p. 3006.
36. Jaschinski, B., Blachnik, R., Pawlak, R., and Reuter, H., *J. Kristallogr. NCS*, 1998, vol. 213, nos. 1–4, p. 541.
37. Savilov, S., Kloo, L., Kuznetsov, A., et al., *Z. Anorg. Allg. Chem.*, 2003, vol. 629, no. 14, p. 2525.
38. Gerasimenko, A.V., Karaseva, E.T., and Polishchuk, A.V., *Acta Crystallogr., Sect E: Structure Reports Online,* 2008, vol. 64, no. 2, p. m378.
39. Alcock, N.W., *Adv. Inorg. Chem. Radiochem.*, 1972, vol. 15, no. 1, p. 1.
40. Uson, R., Laguna, A., Laguna, M., et al., *Chem. Commun.*, 1988, no. 11, p. 740.
41. Pathaneni, S.S. and Desiraju, G.R., *J. Chem. Soc., Dalton Trans.*, 1993, no. 2, p. 319.
42. Schmidbaur, H., *Gold Bull.*, 2000, vol. 33, no. 1, p. 3.
43. Haiduc, I. and Edelmann, F.T., *Supramolecular Organometallic Chemistry*, Cambridge: Wiley, 1999.
44. Razuvaev, G.A., Almazov, G.V., Domrachev, G.A., et al., *Dokl. Akad. Nauk SSSR*, 1987, vol. 294, no. 1, p. 141.
45. Lidin, R.A., Andreeva, L.L., and Molochko, V.A., *Spravochnik po neorganicheskoi khimii* (Handbook in Inorganic Chemistry), Moscow: Khimiya, 1987.
46. Larionov, S.V., Mikhalin, I.N., Glinskaya, L.A., et al., *Russ. J Inorg. Chem.*, 2004, vol. 49, no. 3, p. 331.
47. Ptaszynski, B., Skiba, E., and Krystek, J., *J. Therm. Anal. Calorim.*, 2001, vol. 65, no. 1, p. 231.
48. Ripan, R. and Ceteanu, I., *Chimia Metalelor*, Bucuresti: Editura Didactica si Pedagogica, 1968, vol. 1.

Translated by Z. Svitanko